Possible association of G6PC2 and MUC6 induced by low-dose-rate irradiation in mouse intestine with inflammatory bowel disease

SOHI KANG[1,2*], MIN JI BAE[3*], MIN KOOK KANG[3], HYOJIN KIM[3], YEONG-ROK KANG[3], WOL SOON JO[3], CHANG GEUN LEE[3], BOKYUNG JUNG[1], JEONGMIN LEE[1], CHANGJONG MOON[1], YEONGHOON SON[4], HAE-JUNE LEE[4] and JOONG SUN KIM[1]

[1]College of Veterinary Medicine and BK21 FOUR Program, Chonnam National University, Gwangju 61186; [2]Department of Anatomy and Convergence Medical Science, College of Medicine, Institute of Health Sciences, Gyeongsang National University, Jinju, South Gyeongsangnam-do 52727; [3]Research Center, Dongnam Institute of Radiological & Medical Sciences (DIRAMS), Busan 46033; [4]Division of Radiation Biomedical Research, Korea Institute of Radiological & Medical Sciences (KIRAMS), Seoul 01812, Republic of Korea

Received October 12, 2023; Accepted April 2, 2024

DOI: 10.3892/mmr.2024.13251

Abstract. Although there are several types of radiation exposure, it is debated whether low-dose-rate (LDR) irradiation (IR) affects the body. Since the small intestine is a radiation-sensitive organ, the present study aimed to evaluate how it changes when exposed to LDR IR and identify the genes sensitive to these doses. After undergoing LDR (6.0 mGy/h) γ radiation exposure, intestinal RNA from BALB/c mice was extracted 1 and 24 h later. Mouse whole genome microarrays were used to explore radiation-induced transcriptional alterations. Reverse transcription-quantitative (RT-q) PCR was used to examine time- and dose-dependent radiation responses. The histopathological status of the jejunum in the radiated mouse was not changed by 10 mGy of LDR IR; however, 23 genes were upregulated in response to LDR IR of the jejunum in mice after 1 and 24 h of exposure. Upregulated genes were selected to validate the results of the RNA sequencing analysis for RT-qPCR detection and results showed that only Na^+/K^+ transporting subunit α4, glucose-6-phosphatase catalytic subunit 2 (G6PC2), mucin 6 (MUC6) and transient receptor potential cation channel subfamily V member 6 levels significantly increased after 24 h of LDR IR. Furthermore, G6PC2 and MUC6 were notable genes induced by LDR IR exposure according to protein expression via western blot analysis. The mRNA levels of G6PC2 and MUC6 were significantly elevated within 24 h under three conditions: i) Exposure to LDR IR, ii) repeated exposure to LDR IR and iii) exposure to LDR IR in the presence of inflammatory bowel disease. These results could contribute to an improved understanding of immediate radiation reactions and biomarker development to identify radiation-susceptible individuals before histopathological changes become noticeable. However, further investigation into the specific mechanisms involving G6PC2 and MUC6 is required to accomplish this.

Correspondence to: Professor Joong Sun Kim, College of Veterinary Medicine and BK21 FOUR Program, Chonnam National University, 77 Yongbong, Buk-gu, Gwangju 61186, Republic of Korea
E-mail: centraline@jnu.ac.kr

Dr Hae-June Lee, Division of Radiation Biomedical Research, Korea Institute of Radiological & Medical Sciences (KIRAMS), 75 Nowon-ro, Nowon, Seoul 01812, Republic of Korea
E-mail: hjlee@kirams.re.kr

*Contributed equally

Key words: low-dose-rate radiation, intestine, inflammatory bowel disease, glucose-6-phosphatase catalytic subunit 2, mucin 6

Introduction

Our bodies are exposed to radiation in numerous ways, in both high and low doses. The systemic effect of radiation is directly related to dosage quantity and rate (1). Normal cells are also damaged by high-dose radiation resulting from accidental radiation leaks, with detrimental effects on the quality of life in survivors (2). Several research teams are attempting to identify compounds that can protect radiosensitive organs, such as the testis (3), intestines (4) and hippocampus (5). However, there is controversy about how low-dose radiation exposure (≤0.2 Gy) (6), such as that from imaging diagnosis (X-ray or computed tomography scan), affects the health of patients (7,8). Previous studies showed that low-dose rate (LDR) irradiation (IR) induces testicular damage (9) and aggravates nanoparticle-induced lung injury (10). However, several findings also suggest that low-dose radiation ameliorates asthma symptoms (11) and delays the progression of Alzheimer's disease (12). In particular, the relationship between cumulative radiation dose and unfavorable effects, predicated on ongoing, LDR IR exposure, has not been fully explained.

The gastrointestinal system is extremely sensitive to radiation (13). Most radiation enteritis, or radiation-induced

intestinal damage, occurs during abdominopelvic radiotherapy (14). Patients with radiation enteritis initially experience diarrhea, stomach pain and weight loss; however, as the condition progresses, cancer eventually develops (15). Studies on low-dose radiation resulting in radiation enteritis are still inconclusive, with uncertainty on induced alterations.

Finding genes sensitive to low-dose radiation can provide insights into how LDR radiation affects the human body. RNA sequencing (RNA-seq) provides an unbiased screening strategy for potential novel biomarkers associated with radiation response when searching for a predictor of response. The present study examined the crucial genes that could be linked to the radiation-induced intestinal injury response to LDR IR exposure.

Materials and methods

Animals. A total of 90 6-week-old female (weight, 18-21 g) BALB/c mice were obtained from Dooyeol Biotech and housed at 23±2˚C and relative humidity of 50±5%, with artificial illumination from 08:00-20:00 and 13-18 air changes per h. The mice were classified into three main categories: control, LDR IR 1 h before, and LDR IR 24 h before. The mice were housed in groups (n=3 mice per group) and received standard laboratory feed and water at all times. The experiment involved continuous monitoring of animal health and behavior, conducted twice daily. All experimental procedures were conducted according to the National Institutes of Health Guide for the Care and Use of Laboratory Animals (NIH Publications No. 8023, 8th edition, revised 2011) (16) and a protocol approved by the Institutional Animal Care and Use Committee of the Dongnam Institute of Radiological and Medical Sciences (DIRAMS; approval nos. DI-2015-002 and DI-2021-002).

Efforts were made to reduce suffering and distress among the animals by providing analgesics (xylazine; Rompun®; 10 mg/kg; Bayer Koreaa; via intraperitoneal injection) or anesthetics (alfaxalone; 85 mg/kg (17); Jurox Pty Ltd.; via intraperitoneal injection) as needed as well as establishing certain housing conditions. If experimental animals exhibited visible alterations as well as a weight loss >20%, they were sacrificed in accordance with criteria for humane endpoints. Following the administration of respiratory anesthetic induction using 5% isoflurane for 60 sec, the mouse appeared to be in an unconscious state. The dose rate of isoflurane was reduced by 2% for maintenance anesthesia and euthanasia was carried out by applying a cervical dislocation. Death was confirmed through a physical examination, which revealed the absence of the cardiac and respiratory activity. A total of 90 mice were used in the experiments. No mice were euthanized due to humane endpoints and no mice were found dead throughout the experiment.

Radiation exposure. The LDR IR exposure was similar to that previously described (10,11). The DIRAMS LDR IR facility used radiation exposure with a ^{137}Cs source (370 GBq). The mouse cages were positioned on shelves with dose rates of 6.0 mGy/h; the total accumulative radiation dose of the set-up places was 10, 100 and 500 mGy. The group exposed to LDR IR at 10 mGy undergo three exposures, each occurring at intervals of 3 days. In addition, mice were high-dose rate (HDR) irradiated with a single 500 mGy dose using 6 MV high energy photon rays (Elekta Instrument AB) at 3.8 Gy/min. Sham-irradiated mice were treated similarly but without radiation. After 1 and 24 h of irradiation, the mice were sacrificed and intestinal tissue samples were taken.

Histological analysis. The small intestine was fixed in 10% neutral buffered formaldehyde for 24 h at room temperature and four distinct jejunal segments were sliced into 4 μm thick pieces and placed on glass slides. To examine morphology, jejunal slices were stained with hematoxylin and eosin for 2 and 1 min at room temperature. All samples were sectioned and reoriented in successive slices to examine the morphological alterations and ascertain which ones had the longest villi. This method was chosen because it produced more reliable results than standard techniques, which only measured the 10 longest villi in a single slice per sample (4,18). A total of 10 jejunal sections, including the height of the basal lamina and the length of the 10 longest villi, were measured from each animal. The stained sections were analyzed using a Motic Easyscan Digital Slide Scanner (Motic Incorporation, Ltd.).

Dextran sulfate sodium (DSS)-induced colitis. The induction of colitis in murine models by DSS (cat. no. 160110; 36-50 kDa; MP Biomedicals) was similar to that previously described (19); 5% DSS dissolved in drinking water was used as the treatment method for mice for 7 days. In the control groups, mice were given normal drinking water.

Total RNA and mRNA Isolation. Mice (n=1 mouse per group) were sacrificed and their jejunum tissue were removed. TRIzol® reagent (cat. no. 15596026; Thermo Fisher Scientific, Inc.) was used for total RNA extraction, according to the manufacturer's instructions. RNase-Free DNase I (cat. no. EN0521; Thermo Fisher Scientific, Inc.) was used to degrade genomic DNA. Total RNA levels in the samples were measured using a Nanodrop 2000 spectrophotometer (Thermo Fisher Scientific, Inc.). BioAnalyzer2100 (Agilent Technologies, Inc.) analyzed sample size, quantification and integrity, eliminating those with a RNA integrity number <7. Following the manufacturer's instructions, NEXTflex Poly (A) Beads (Bioo Scientific Corp.) was used to isolate mRNA from total RNA samples.

mRNA sequencing library preparation and sequencing. The NEXTflex Rapid Directional RNA-Seq Library Prep Kit 2.0 (Bioo Scientific Corp.) was used to create an RNA sequencing library in accordance with the manufacturer's protocols. In brief, mRNA was chemically fragmented after isolation from 1 μg of total RNA using NEXTflext Poly (A) Beads. Following the creation of the double-stranded cDNA from the fragmented mRNA, the library was purified using magnetic beads made by Agencourt AMPure XP (Beckman Coulter, Inc.), 3'-end adenylation and sequencing adapter ligation. The experiment used the Agilent 2100 Bioanalyzer and reverse transcription-quantitative (RT-q) PCR to verify each library's successful preparation before moving on to massively parallel deep sequencing. HiSeq 2500 sequencing platform (Illumina, Inc.) was used for paired-end sequencing with a typical read

size of 100 nucleotides. The Illumina base-calling pipeline processed the raw sequencing data and two technical duplicates were created and sequenced for every sample.

Transcriptome mapping and data analysis. Adaptor and low-quality bases were trimmed with Cutadapt ver. 1.3 (20) and Trim Galore ver. 0.44 (https://www.bioinformatics.babraham.ac.uk) and the clean reads were aligned to the reference rat genome (rn5) downloaded from Ensemble (www.ensembl.org) with STAR ver. 2.5 (21). Mapped data from the bam file was imported to StrandNGS ver. 2.9 (StrandNGS.com) for further expression analysis. Gene quantitation was normalized using DESEQ (22) and baseline correction to the median of gene expression and log2 transform were applied. Differentially expression genes (DEGs) were determined by log2-transformed fold changes (≥1 or ≤-1) with one-way analysis of variance (ANOVA; false discovery rate <0.1). To investigate Gene ontology (GO) enrichment of DEGs, we utilized Homer ver. 4.5 (23) and Metascape webserver (http://metascape.org) (24), with *Mus musculus* used as the input species and analyzed GO biological process (GO:BP) dataset to identify upregulated genes. Only terms meeting the criteria of P<0.05, a minimum count of 3 and an enrichment factor >2 was considered significant. The most statistically significant term in a cluster was selected to represent that cluster.

RT-qPCR analysis. Using an ISOGEN kit (311-02501; Nippon Gene, Tokyo, Japan), total RNA was isolated from jejunal samples. RT-qPCR analyses were performed as described in a previous study (4). RT-qPCR was performed duplicate using CFX Opus 96 instrument (Bio-Rad Laboratories) and TOPreal™ SYBR Green qPCR 2x PreMIX (Cat. No. RT500M; Enzynomics) and the according the manufacturer's guidelines. The RT-qPCR reaction was carried out in a 25 μl reaction, including 5 μl of cDNA (40 ng), 1 μl of each primer (6 μM), 12.5 μl of 2x SYBR green PreMix, and 5.5 μl of double distilled water. The thermal cycling profile comprised a preincubation step at 94˚C for 10 min, followed by 45 cycles of denaturation (94˚C, 15 sec), annealing (55-60˚C, 30 sec), and elongation (72˚C, 20 sec). The software generated amplification curves and determined threshold cycle values. Primer candidates were acquired utilizing an application available on the PRIMER3 ver. 0.4.0 website (https://bioinfo.ut.ee/primer3-0.4.0/). The primers were validated using the NCBI BLAST (basic local alignment search tool) ver. +2.15.0 database (https://blast.ncbi.nlm.nih.gov/). The expression levels of mRNAs for ATPase NA^+/K^+ transporting subunit alpha 4 (ATP1A4), glucose-6-phosphatase catalytic subunit 2 (G6PC2), mucin 6 (MUC6), mucin 20 (MUC20) and transient receptor potential cation channel subfamily V member 6 (TRPV6) were measured, normalized to the expression level of glyceraldehyde-3-phosphate dehydrogenase (GAPDH) mRNA expression and expressed relative to the corresponding mean value for the jejunum tissue of control mice that was unexposed to radiation using the $2^{-\Delta\Delta Cq}$ method (25). Mouse primers used in analysis were as follows: ATP1A4-(NM_013734) forward 5'-CTGGTGAGCTGAATCAGAAACC-3' and reverse 5'-AAGACCCTTGGTCAAGTCCAC-3'; G6PC2-(NM_001289857) forward 5'-CAGGAGGACTACCGGACTTAC-3' and reverse 5'-TCAACTGAAACCAAAGTGGGAA-3'; MUC6-(NM_001368953) forward 5'-AGCCCACATTCCCTATCAGC-3' and reverse 5'-CACAGTGGAAGATTGCGAGAG-3'; TRPV6-(NM_022413) forward 5'-AGGGGTTAATACTCTGCCTATGG-3' and reverse, 5'-GCACCTCACATCCTTCAAACTT-3'; GAPDH-(NM_008084.2) forward 5'-TCCATGACAACTTTGGCATT-3' and reverse 5'-GTTGCTGTTGAAGTCGCAGG-3'.

Western blot analysis. The jejunum was homogenized in buffer H (50 mM β-glycerophosphate, 1.5 mM ethylene glycol tetra acetic acid, 0.1 mM Na_3VO_4, 1 mM dithiothreitol, 10 μg/ml aprotinin, 2 μg/ml pepstatin, 10 μg/ml leupeptin, and 1 mM phenylmethanesulfonyl fluoride, pH 7.4) for western blotting examination. The protein content of each sample was determined using a Bio-Rad protein assay reagent (cat. no. 500-0006; Bio-Rad Laboratories, Hercules, CA, USA). Western blotting was performed as described previously (10). Briefly, each sample's total protein equivalent was separated on 10% SDS-polyacrylamide gels (40 μg of protein per lane) and transferred to an Immobilon-PSQ transfer membrane (cat. no. ISEQ00010; MilliporeSigma). The membrane was soaked for 1 h at room temperature in a blocking solution containing 5% non-fat milk. Primary antibodies against ATP1A4 (diluted 1:1,000; cat. no. STJ117451; St John's Laboratory Ltd.), G6PC2 (diluted 1:1,000; cat. no. bs-13386R; BIOSS), MUC6 (diluted 1:1,000; cat. no. 224329; United States Biological) and TRPV6 (diluted 1:1,000; cat. no. ACC-036; Alomone Labs) were incubated at 4˚C with consistent rocking overnight. After four 10-min Tris-buffered saline (TBS) and 0.1% Tween-20 (TBS-T) washes, the membrane was incubated with secondary polyclonal anti-rabbit antibodies (diluted 1:10,000; cat. no. 12-348; MilliporeSigma) in TBS-T buffer at ambient temperature for 1 h. Using a chemiluminescence reagent (cat. no. 34580; SuperSignal West Pico PLUS; Thermo Fisher Scientific) and the ChemiDoc MP Imaging system (Bio-Rad Laboratories, Inc.), the labeling of the secondary antibody conjugated with horseradish was detected. The membrane was probed with β-actin (diluted 1:5,000; cat. no. A5441; MilliporeSigma), a housekeeping gene, to measure protein expression levels. Using Image Lab ver. 6.0.1 (Bio-Rad Laboratories, Inc.) software, protein bands were quantified.

Statistical analysis. Results are presented as mean ± standard error of mean (SEM). Radiation-induced response screening was analyzed using one-way analysis of variance (ANOVA) with additional Tukey's post hoc testing. Dose-dependent response validation, frequency-dependent response validation and evaluation of correlation between LDR IR and inflammatory bowel disease (IBD) were analyzed using two-way ANOVA followed by Tukey's post hoc testing. P<0.05 was considered to indicate a statistically significant difference.

Results

Gene ontology biological process analysis of RNA-seq screening data. To screen for genes changed by LDR IR exposure, RNA-seq was performed 1 and 24 h after irradiation at 10 mGy (Fig. 1A). At 1 h following radiation exposure, 12 enriched GO:BP terms were obtained when 0 Gy was compared with 1 h after exposure to 10 mGy (Fig. 1B and

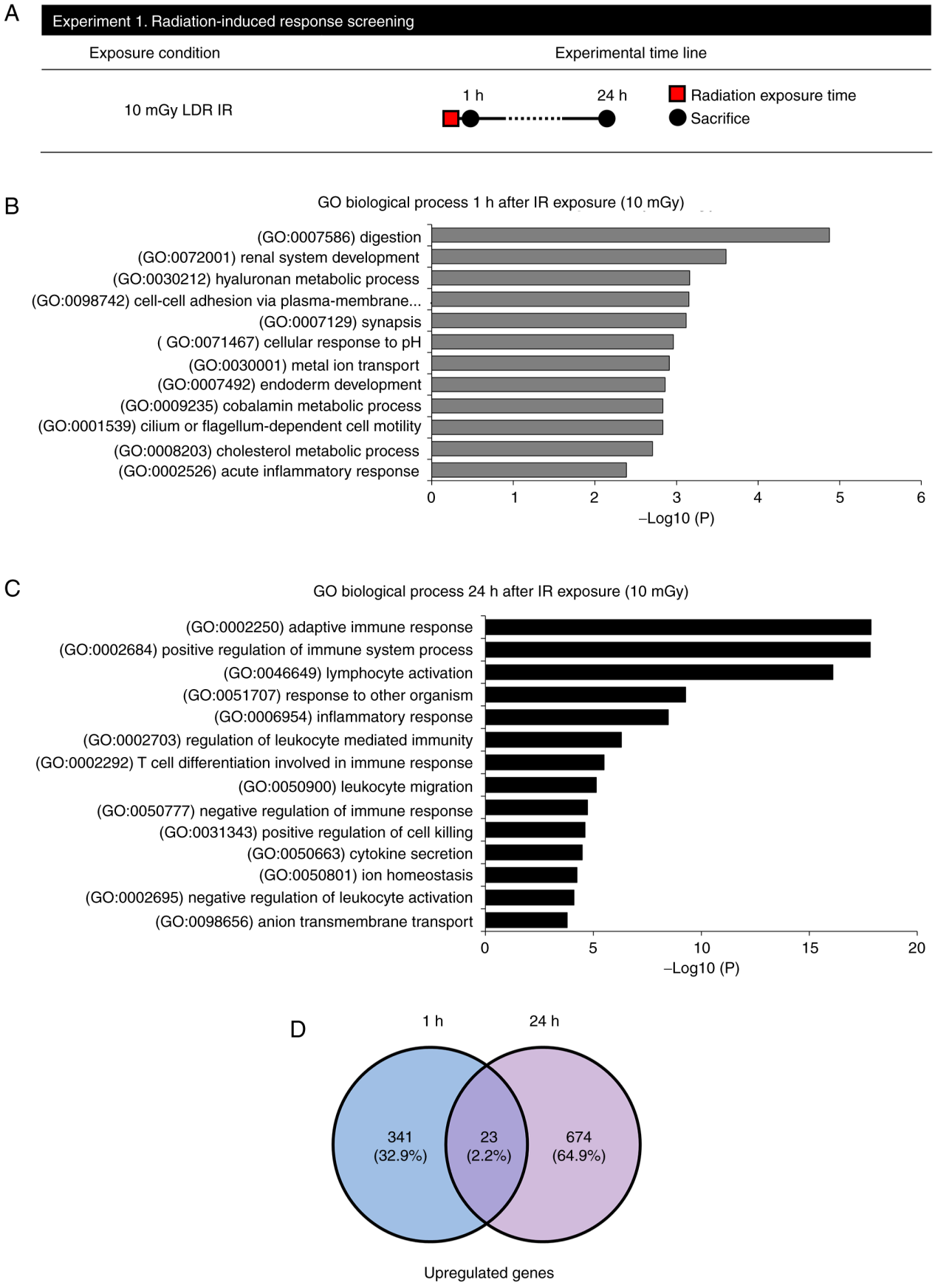

Figure 1. (GO) analysis of RNA-seq screening data. (A) Schematic diagram of the experimental procedure. In experiment 1, mice irradiated with sham (0 Gy) or 10 mGy were sacrificed for tissue sampling at 1 or 24 h following LDR IR. Red square indicates radiation exposure time; black circles indicate the times of tissue collection from test animals. Functional enrichment analysis of DEGs. GO biological process enrichment analysis of upregulated DEGs in jejunal tissue at (B) 1 h and (C) 24 h following LDR radiation. Bar graphs show the relative expression levels of upregulated genes from RNA-seq data. (D) Venn diagram illustrating the number of significant DEGs in the 1 and 24 h after low-dose rate irradiation. GO, Gene Ontology; RNA-seq, RNA-sequencing; LDR IR, low-dose-rate irradiation; DEGs, differentially expressed genes.

Table I. GO term enrichment analysis of DEGs 1 h after 10 mGy radiation exposure.

Pathways	P-value	DEGs/Total	Genes
(GO:0007586) digestion	$1.34x10^{-5}$	10/164	AMY2A, AMY2B, CCKAR, CEL, CLPS, CTRL, MUC6, PPY, PRSS3, WNK3
(GO:0072001) renal system development	$2.47x10^{-4}$	13/277	HMGCS2, LHX1, NPHS1, PKHD1, UMOD, TBX18, CRLF1, KLHL3, KLF15, SIX4, PKD1L3, FZD3, RNF207
(GO:0030212) hyaluronan metabolic process	$6.48x10^{-4}$	4/37	EGF, ITIH2, ITIH4, HYAL3
(GO:0098742) cell-cell adhesion via plasma-membrane adhesion molecules	$7.04x10^{-4}$	20/219	FAT2, UMOD, PCDHGB4, CLDN10, PCDHGC5, PCDHGB5, PCDHGB1, PCDHGA4, CDHR4, CEL, CTLA4, IGFBP2, INS, ITGA2B, PKHD1, CCL2, EOMES, MMP24, CLEC4E, ADGRV1
(GO:0007129) synapsis	$7.63x10^{-4}$	4/38	SYCP2, STAG3, SPO11, RNF212
(GO:0071467) cellular response to pH	$1.06x10^{-3}$	3/19	INSRR, SLC38A3, PKD1L3
(GO:0030001) metal ion transport	$1.23x10^{-3}$	21/796	ATP1A4, CCKAR, CNGA1, EGF, KCNJ11, SCN4A, CCL2, SLC12A3, SLC38A3, KLHL3, SLC40A1, TRPV6, WNK3, CATSPER2, KCNH8, SLC9B2, NKAIN2, PKD1L3, RNF207, CPT1B, CHRNA2
(GO:0007492) endoderm development	$1.38x10^{-3}$	6/75	COL7A1, ONECUT1, LHX1, VTN, EOMES, CRB2
(GO:0009235) cobalamin metabolic process	$1.48x10^{-3}$	3/21	PRSS3, CUBN, CTRC
(GO:0001539) cilium or flagellum-dependent cell motility	$1.48x10^{-3}$	3/21	DNAH6, DNAH7, CFAP54
(GO:0008203) cholesterol metabolic process	$1.97x10^{-3}$	10/119	CEL, HMGCS2, STAR, CUBN, CELA3B, APOL2, ALDH3A1, CCKAR, IGFBP2, CCL2
(GO:0002526) acute inflammatory response	$4.12x10^{-3}$	11/138	C4B, INS, ITIH4, VTN, APOL2, NUPR1, COL7A1, ITIH2, SSPO, SERPINA10, CRB2

GO, Gene Ontology; DEGs, differentially expression genes.

Table I). Furthermore, there was an increase in the BP associated with the digestion system. After 24 h of radiation exposure, 14 enriched GO:BP terms were obtained when 0 Gy was compared with 24 h after 10 mGy (Fig. 1C and Table II). Moreover, there was an observed increase in the BP associated with the immune system. However, no meaningful biological process demonstrated an expected increase across a period of 1 and 24 h following exposure. RNA-seq was used to find genes responsive to LDR IR exposure to identify DEGs affected in the LDR IR jejunum (364 DEGs upregulated in the 1 h after LDR irradiated jejunum; 697 DEGs upregulated in the 24 h after LDR of the jejunum, with 23 genes in common with the comparison of 1 and 24-h IR groups; Fig. 1D and Table III).

Immediately following LDR IR exposure, G6PC2 and MUC6 mRNA and protein expression are increased. To verify changes in genes and proteins caused by LDR IR exposure, RT-qPCR and western blot were performed on mice 1 and 24 h after irradiation at 10 mGy (Fig. 2A). A total of 23 DEGs were selected for qPCR detection to validate the outcome of RNA-seq analysis: APOL2, ATP1A4, CCL2, CCL20, CLEC4E, CRLF1, G6PC2, INS, ITIH4, KLHL3, MUC20, MUC6, NPHS1, PPY, REG1B, SERPINA10, SLC40A1, SLC9B2, SPX, TNFRSF8, TRPV6, UMOD and WNK3. Among these, qPCR results showed that only ATP1A4, G6PC2, MUC6 and TRPV6 levels increased significantly 24 h after LDR IR (Fig. 2B). The protein expression levels of ATP1A4, G6PC2, MUC6, MUC20 and TRPV6 were examined (Fig. 2C and D). G6PC2 expression showed significant upregulation in the 1 and 24 h following 10 mGy radiation exposure to the jejunum. MUC6 was also significantly upregulated in the 24 h following LDR IR exposure. However, MUC20 was not detectable by western blotting and ATP1A4 and TRPV6 did not alter after LDR IR exposure. Therefore, it was hypothesized that G6PC2 and MUC6 are important genes triggered by LDR IR exposure.

G6PC2 mRNA increases in low doses of LDR IR and repeated LDR IR exposure conditions in the jejunum. To further validate the dose-dependent change in G6PC2 gene expression, qPCR analysis was performed on mice intestinal tissues exposed to LDR IR (10, 100 and 500 mGy) and HDR (500 mGy; Fig. 3A). In the jejunum, G6PC2 gene expression was significantly increased following 10 and 100 mGy exposure compared with the sham group (Fig. 3B). However, 500 mGy of LDR IR and 500 mGy of HDR IR did not alter G6PC2 expression

Table II. GO term enrichment analysis of DEGs 24 h after 10 mGy radiation exposure.

Pathways	P-value	DEGs/Total	Genes
(GO:0002250) adaptive immune response	$1.40x10^{-18}$	76/371	BTK, C4B, CD27, CD40, CD79B, CLU, CR2, CTLA4, CD55, FCER2, IGHD, IGHG1, IGHM, IGLC2, IL12A, JAK3, LY9, POU2F2, CCL19, SLAMF1, TNF, LAT2, EOMES, IL27RA, MASP2, LILRB4, CLCF1, LAT, SIT1, FOXP3, LEF1, IL20RB, LAX1, LIME1, AICDA, MYO1G, FCAMR, KLHL6, SLAMF6, TNFRSF13C, BTLA, CLEC4D, THEMIS, KLRD1, NOS2, CCL2, STAP1, IL21, CA7, IFI16, IL2RA, INS, MX1, MYLK, PPY, MYOM1, CHST3, TSPAN32, CLEC4E, ALPK1, NLRC5, PGLYRP2, TRIM6, CXCR5, MS4A1, IKZF3, BANK1, TNIP2, CCR6, LTF, PAX5, SERPINC1, F8, ABCA1, PRTN3, MARCO
(GO:0002684) positive regulation of immune system process	$1.49x10^{-18}$	74/943	BTK, C4B, CD2, CD19, CD27, CD40, CD79B, CLU, CCR6, MAP3K8, CR2, CTLA4, CD55, COCH, FCER2, CXCL1, CXCL2, IFI16, IGHD, IGHG1, IGHM, IGLC2, IL2RA, IL12A, ITGA2B, JAK3, LTF, NOS2, CCL2, CCL19, CCL20, CXCL5, SLAMF1, TNF, LAT2, MARCO, IL27RA, MASP2, CLCF1, STAP1, CLEC4E, LAT, ICOS, FOXP3, LEF1, UBASH3A, LAX1, LIME1, IL21, TRPV4, MYO1G, RASAL3, TNIP2, TNIP3, FCRL5, NLRC5, KLHL6, PGLYRP2, SLAMF6, TNFRSF13C, TRIM6, REG3G, SLC9B2, CARMIL2, BTLA, GCSAM, CLEC4D, ABCB5, TICAM2, THEMIS, RASAL1, RASGRP3, SPTBN5, IL20RB
(GO:0046649) lymphocyte activation	$8.02x10^{-17}$	103/618	CXCR5, BTK, CD2, MS4A1, CD27, CD40, MAP3K8, CR2, CTLA4, CD55, HLA-DOA, IGHD, IGHG1, IGHM, IGLC2, IL2RA, IL12A, INS, JAK3, LY9, POU2F2, SATB1, CCL2, CCL19, SLAMF1, LAT2, EOMES, IL27RA, IKZF3, KIAA0922, CLCF1, CLEC4E, LAT, SIT1, ICOS, IL21R, FOXP3, LEF1, IL20RB, LAX1, BANK1, AICDA, IL21, RASAL3, TNIP2, NFKBID, PGLYRP2, SLAMF6, TNFRSF13C, CARMIL2, BTLA, CLEC4D, THEMIS, CLU, CNR2, TSPAN32, STAP1, F8, ITGA2B, PLEK, TTN, SLC7A11, C6orf25, CELSR3, REG3A, S100A9, TNF, UMOD, PCDHGB4, PCDHGC5, PCDHGB5, PCDHGB1, PCDHGA7, PCDHGA4, TRPV4, CDH26, PCDH15, ADGRV1, CDHR4, IFI16, LTF, PRTN3, LILRB4, SLC9B2, APOD, HLA-DOB, UBASH3A, FCRL5, NLRC5, GCSAM, TICAM2, ABCA1, ALOX15B, TNFRSF8, LTB, NOS2, CCL20, WNT11, TRIM6, SLC40A1, SIX4, NUGGC, RELL2
(GO:0051707) response to other organism	$5.33x10^{-10}$	71/922	ABCA1, C4B, CA7, CD27, TNFRSF8, CD40, CLU, CNR2, CYP27B1, CD55, COCH, CXCL1, CXCL2, HMGCS2, IFI16, IGHD, IGHG1, IGHM, IGLC2, IL2RA, IL12A, LTF, MX1, MYLK, NOS2, PPY, S100A9, CCL2, CCL19, CCL20, CXCL5, STAR, TIMP4, TNF, CXCR4, MYOM1, SOCS3, IL27RA, CHST3, TSPAN32, STAP1, CLEC4E, FOXP3, AICDA, TNIP2, TNIP3, ALPK1, NLRC5, PGLYRP2, TRIM6, REG3G, CLEC4D, TICAM2, IFITM10, APOD, SERPINC1, BTK, MAP3K8, INS, MARCO, IL20RB, IL21, TRPV4, SLAMF6, GIPR, NPY1R, WNT11, NCOA4, GPR83, LEF1, CCDC62
(GO:0006954) inflammatory response	$5.37x10^{-9}$	61/646	APOD, SERPINC1, C4B, CD27, TNFRSF8, CD40, CNR2, CD55, F8, FPR2, CXCL1, CXCL2, IFI16, IL2RA, INS, ITIH4, NOS2, REG3A, S100A9, CCL2, CCL19, CCL20, CXCL5, TNF, CXCR4, NPFF, SOCS3, CHST4, APOL2, LAT, FOXP3, IL20RB, IL21, TRPV4, TNIP2, TNIP3, NFKBID, PGLYRP2, REG3G, TICAM2, PLA2G4B, CA7, CCR6, CNGA1, CYP27B1, IL12A, LTF, MYLK, PDE6G, PLEK, PPY, RHO, MYOM1, CHST3, TSPAN32, STAP1, ALPK1, SPX, TRIM6, ATP6V0D2, NLRC5

Table II. Continued.

Pathways	P-value	DEGs/Total	Genes
(GO:0002703) regulation of leukocyte-mediated immunity	$5.03x10^{-7}$	32/155	BTK, CD40, FCER2, IL12A, JAK3, NOS2, CCL2, SLAMF1, TNF, IL27RA, CLCF1, STAP1, FOXP3, IL20RB, IL21, SLAMF6, CCL19, TNFRSF13C, CD55, POU2F2, VPREB3, LAX1, AICDA, TRIM6, NUGGC, MS4A1, CR2, CTLA4, IKZF3, LEF1, CRLF1, TEX15
(GO:0002292) T cell differentiation involved in immune response	$3.16x10^{-6}$	24/54	JAK3, LY9, CCL19, EOMES, CLEC4E, FOXP3, LEF1, SLAMF6, CLEC4D, CD55, IL12A, INS, SATB1, RASAL3, CD40, SLAMF1, LAT2, IL27RA, CLCF1, LAT, AICDA, PGLYRP2, IL21, THEMIS
(GO:0050900) leukocyte migration	$7.22x10^{-6}$	18/355	APOD, CD2, CCR6, CXCL1, CXCL2, IL12A, ITGA2B, MAG, S100A9, CCL2, CCL19, CCL20, CXCL5, SELL, TNF, UMOD, CXCR4, SLC7A1
(GO:0050777) negative regulation of immune response	1.85×10^{-5}	20/120	CD55, IFI16, IL2RA, INS, JAK3, SLAMF1, TNF, IL27RA, FOXP3, IL20RB, NLRC5, PGLYRP2, BTK, CD40, CLCF1, TRIM6, SATB1, IL12A, MYO1G, BANK1
(GO:0031343) positive regulation of cell killing	$2.42x10^{-5}$	7/39	FCER2, IL12A, NOS2, CCL2, STAP1, IL21, SLAMF6
(GO:0050663) cytokine secretion	$3.27x10^{-5}$	45/169	ABCA1, ALOX15B, CD2, INS, NOS2, CCL19, SLAMF1, TNF, CLEC4E, FOXP3, BANK1, TRPV4, TRIM6, CARMIL2, CD40, CLU, F8, GIPR, ITGA2B, NPY1R, PLEK, POU2F2, PPY, SLC1A7, TFR2, TRPM2, TTN, LAT2, SYN3, NPFF, CACNA1I, LAT, SERPINA10, CKLF, LAX1, TRPV6, G6PC2, MYO1G, SYT8, ILDR1, CYP4A11, NPHS1, S100A9, WNK3, SPX
(GO:0050801) ion homeostasis	$5.66x10^{-5}$	60/664	ABCA1, ATP1A4, CA7, CD40, CCR6, CYP4A11, CYP27B1, CD55, GIPR, INS, JAK3, LTF, NPY1R, RYR1, S100A9, CCL2, CCL19, TFR2, TRPM2, UMOD, CXCR4, NPFF, KLHL3, SLC40A1, TRPV4, WNK3, SPX, FCRL5, SLC4A11, SLC9A7, ATP6V0D2, SLC26A11, CNGA1, GRM6, KCNJ15, MYLK, SCN4A, SCN8A, SLC13A1, CACNA1I, CACNG4, TRPV6, KCNT1, DPP10, SLC13A3, MFSD4B, CATSPER2, SLC9B2, SLC38A8, PKD1L3, CATSPER3, CLCN1, CPT1B, GABRA1, GABRE, SLC37A2, APOC4, AQP9, STAR, G6PC2
(GO:0002695) negative regulation of leukocyte activation	$7.94x10^{-5}$	17/139	CNR2, CTLA4, IL2RA, JAK3, TSPAN32, KIAA0922, FOXP3, IL20RB, LAX1, BANK1, NFKBID, PGLYRP2, LTF, LILRB4, LEF1, TRPV4, CARMIL2
(GO:0098656) anion transmembrane transport	$1.60x10^{-4}$	31/245	ABCA1, AQP9, CLCN1, CPT1B, GABRA1, GABRE, SLC1A7, SLC13A1, SLC7A11, SLC13A3, LRRC8E, SLC4A11, SLC38A8, SLC37A2, SLC26A11, SLC6A18, CA7, CYP4A11, NOS2, PLA2G5, SLCO1C1, ATP8B4, SPX, SLC16A9, APOC4, APOD, CLU, STAR, TNF, APOL2, PLIN5

GO, Gene Ontology; DEGs, differentially expression genes.

levels. Furthermore, G6PC2 expression of the colon also did not change after LDR IR and HDR IR (Fig. 3C). Therefore, it was concluded that G6PC2 only reacts at LDR IR and this reaction is limited to the jejunum. In an additional experiment, the expression level of G6PC2 was validated by repeated LDR IR treatment (Fig. 3D). A single 10 mGy exposure significantly increased G6PC2 expression after 24 h and three 10 mGy exposures increased G6PC2 expression explosively after 24 h (Fig. 3E), suggesting that frequent exposure to LDR effectively increases G6PC2 expression.

MUC6 mRNA increases in low doses of LDR IR and repeated LDR IR exposure conditions in the jejunum. To validate the dose-dependent change in MUC6 gene expression, qPCR analysis was performed on mice intestinal tissue exposed to LDR IR (10, 100 and 500 mGy) and HDR (500 mGy; Fig. 4A). Identifying MUC6 mRNA expression for dose-dependent alterations revealed outcomes comparable to G6PC2. In the jejunum, MUC6 gene expression was significantly higher following 10 mGy exposure compared with the sham group (Fig. 4B). However, 100 and 500 mGy of LDR IR and

Table III. Common upregulated genes.

Gene ID	Gene symbol	Description	Fold change	
			1 h	24 h
239552	APOL2	Apolipoprotein L2	8.3	4.4
480	ATP1A4	ATPase Na+/K+ transporting subunit alpha 4	2.8	3.0
20293	CCL2	C-C motif chemokine ligand 2	3.4	3.5
6364	CCL20	C-C motif chemokine ligand 20	2.1	3.5
26253	CLEC4E	C-type lectin domain family 4 member E	2.1	6.5
9244	CRLF1	Cytokine receptor like factor 1	2.6	2.1
57818	G6PC2	Glucose-6-phosphatase catalytic subunit 2	9.3	8.7
16334	INS	Insulin	140.0	100.0
3700	ITIH4	Inter-alpha-trypsin inhibitor heavy chain family member 4	2.7	6.9
26249	KLHL3	Kelch-like family member 3	3.1	2.3
200958	MUC20	Mucin 20, cell surface associated	4.8	4.9
4588	MUC6	Mucin 6, oligomeric mucus/gel-forming	4.7	6.6
4868	NPHS1	NPHS1 nephrin	3.9	2.5
5539	PPY	Pancreatic polypeptide	29	11
19693	REG1B	Regenerating family member 1 beta	2.3	140
51156	SERPINA10	Serpin family A member 10	8.1	6.3
30061	SLC40A1	Solute carrier family 40 member 1	2.2	3.0
133308	SLC9B2	Solute carrier family 9 member B2	4.3	4.9
80763	SPX	Spexin hormone	5.5	7.2
943	TNFRSF8	Tumor necrosis factor receptor superfamily member 8	11.0	18.0
55503	TRPV6	Transient receptor potential cation channel subfamily V member 6	11.0	11.0
7369	UMOD	Uromodulin	6.5	9.1
65267	WNK3	WNK lysine deficient protein kinase 3	3.7	3.9

500 mGy of HDR IR did not alter MUC6 expression levels. Furthermore, MUC6 expression of the colon also did not change following LDR IR and HDR IR (Fig. 4C). Therefore, it can be concluded that MUC6 only reacts at LDR IR and that this reaction is limited to the jejunum. In an additional experiment, the expression level of MUC6 was validated by repeated LDR IR treatment (Fig. 4D). A single 10 mGy exposure significantly increased MUC6 expression after 24 h and three 10 mGy exposures increased MUC6 expression markedly after 24 h (Fig. 4E), suggesting that frequent exposure to LDR IR effectively increases MUC6 expression.

DSS and LDR IR did not alter jejunal morphology but increased G6PC2 and MUC6 mRNA expression. In order to establish the effect of LDR IR on the intestines with inflammatory conditions, infectious bowel disease was induced by DSS, the jejunal area received radiation and the expression levels of G6PC2 and MUC6 were verified (Fig. 5A). DSS-induced IBD and LDR IR did not cause morphological alterations in the small intestine when processed independently or even after combined treatments; subsequently, neither the length of the villus nor the number of crypts changed, observed 24 h after irradiation (Fig. 5B). Thus, DSS and LDR IR in the jejunum did not act as a powerful stimulus to alter morphological modifications. However, after 24 h, repeated irradiation of LDR IR and DSS significantly boosted G6PC2 expression. Furthermore, when the two stimuli were combined, G6PC2 expression increased with greater efficacy, observed 1 and 24 h after irradiation (Fig. 5C). The expression of MUC6 was significantly increased by exposure to LDR IR and stimulation with DSS. In addition, the combination of these two stimuli led to a substantial increase in MUC6 expression (Fig. 5D).

Discussion

The present study aimed to identify genes that were changed rapidly and consistently in the jejunum of mice exposed to LDR IR. The following important conclusions were noted: i) A total of 23 genes consistently showed elevated expression levels at both 1 and 24 h following exposure to an LDR IR dose of 10 mGy. ii) qPCR and western blot analyses confirmed the expression patterns of the G6PC2 and MUC6 genes. iii) Significantly, the upregulation of G6PC2 and MUC6 gene expressions was limited to the jejunum following exposure to LDR IR, whereas it was not observed in the colon. iv) The increases in the expressions of G6PC2 and MUC6 were more noticeable when exposed to repeated LDR IR, indicating a link between the radiation dosage and the response. v) Furthermore, the present study revealed that in the presence of inflammatory bowel illness, the levels of G6PC2 and MUC6 expressions were increased significantly, emphasizing the possible significance of these genes in developing the disease.

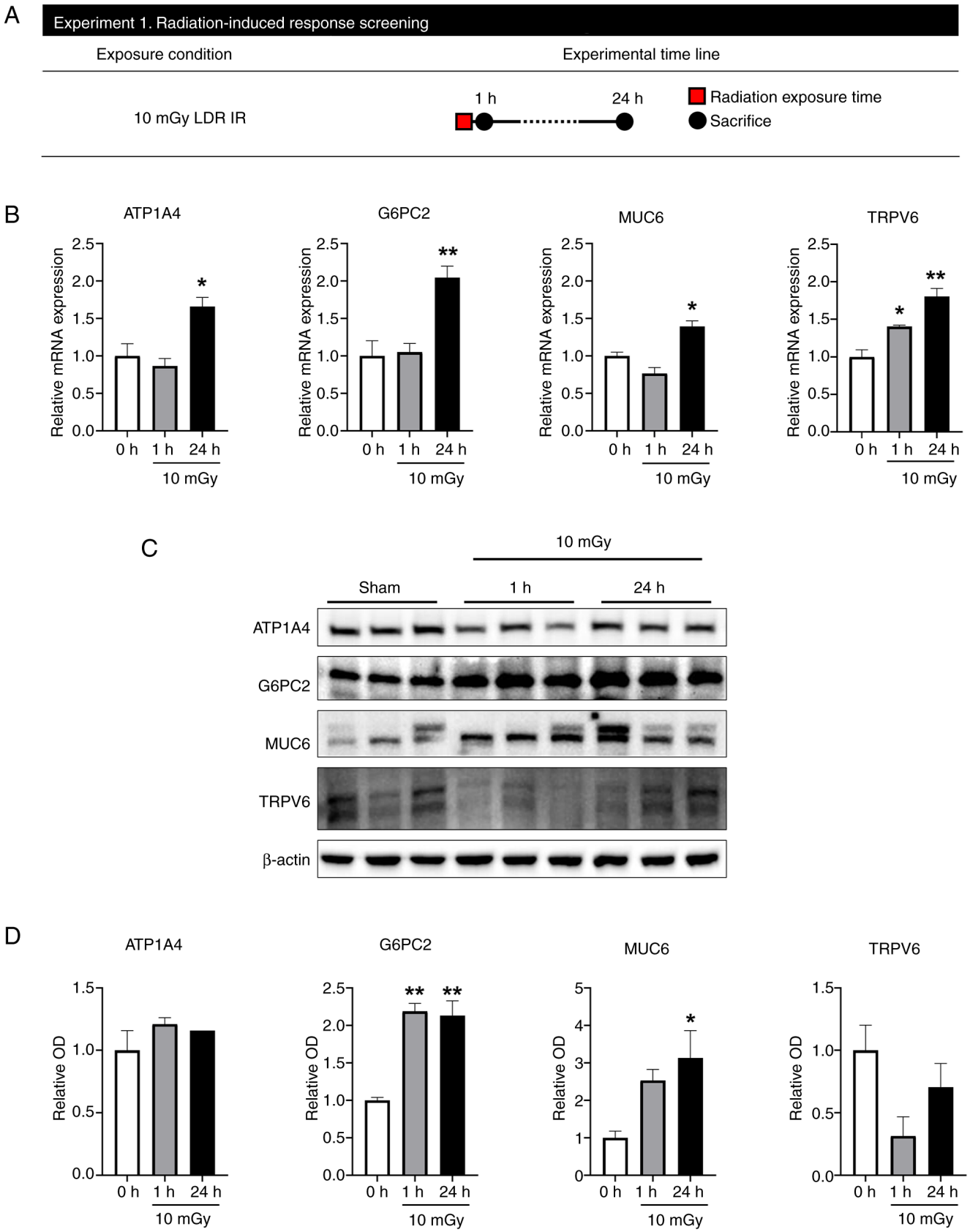

Figure 2. LDR IR increases G6PC2 and MUC6 mRNA and protein expression immediately exposure. (A) Schematic diagram of the experimental procedure. In experiment 1, mice irradiated with sham (0 Gy) or 10 mGy were sacrificed for tissue sampling at 1 or 24 h following LDR IR. Red square indicates radiation exposure time; black circles indicate the times of tissue collection from test animals. Functional enrichment analysis of DEGs. (B) Changes in mRNA expression of four selected genes in the jejunum of mice with LDR IR. Protein expression validation by western blot analysis and temporal changes in protein levels of upregulated genes in 10 mGy-irradiated jejunum. (C) Representative western blotting of ATP1A4, G6PC2, MUC6 and TRPV6 in the jejunum. (D) Bar graphs; expression was normalized to β-actin. Data are expressed as the mean ± SEM (n=3 mice per group). *P<0.05 and **P<0.01 vs. the sham group. LDR IR, low-dose-rate irradiation; G6PC2, glucose-6-phosphatase catalytic subunit 2; MUC6, mucin 6; DEGs, differentially expressed genes; ATP1A4, Na^{+}/K^{+} transporting subunit alpha 4; TRPV6, transient receptor potential cation channel subfamily V member 6.

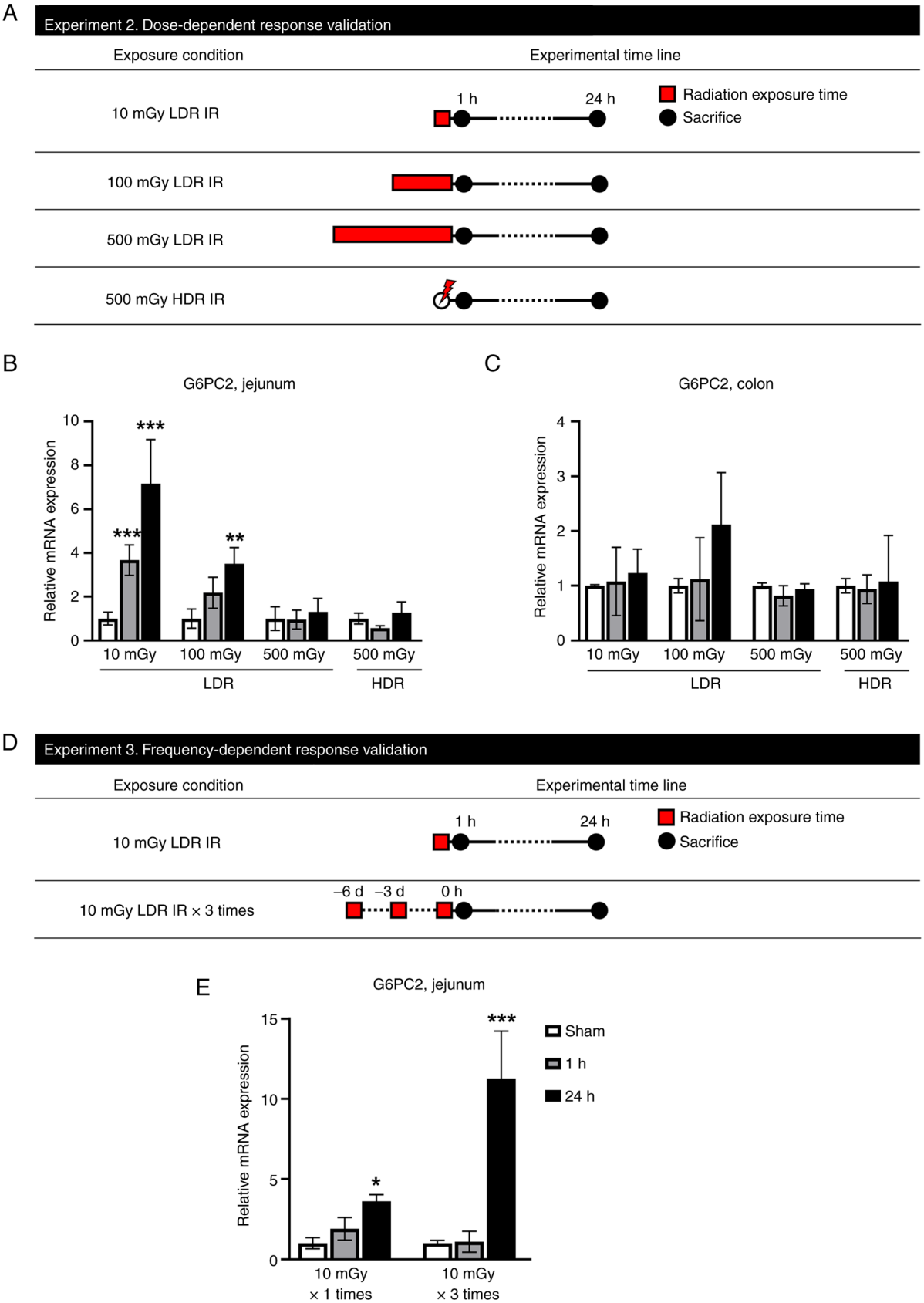

Figure 3. G6PC2 mRNA increases in low dose of LDR IR and repeated LDR IR exposure conditions in the jejunum. (A) Schematic diagram of the experimental procedure. In experiment 2, mice exposed to LDR IR with 0, 10, 100, or 500 mGy or HDR IR with 500 mGy, then sacrificed at 1 or 24 h following IR. Red square indicates radiation exposure time; black circles indicate the times of tissue collection from test animals. Changes in the mRNA expression of G6PC2 in mice exposed to LDR IR. Dose-related changes in G6PC2 mRNA expression level in (B) jejunum and (C) colon. (D) Schematic diagram of the experimental procedure. In experiment 3, mice irradiated with sham, 10 mGy once, or 10 mGy three times were sacrificed for tissue sampling at 1 or 24 h following LDR IR. Red square indicates radiation exposure time; black circles indicate the times of tissue collection from test animals. (E) Repetition-related changes in G6PC2 mRNA expression level in jejunum. Data are expressed as the mean ± SEM (n=3 mice per group). *P<0.05, **P<0.01 and ***P<0.01 vs. the sham group. G6PC2, glucose-6-phosphatase catalytic subunit 2; LDR IR, low-dose-rate irradiation; HDR IR, high-dose-rate irradiation.

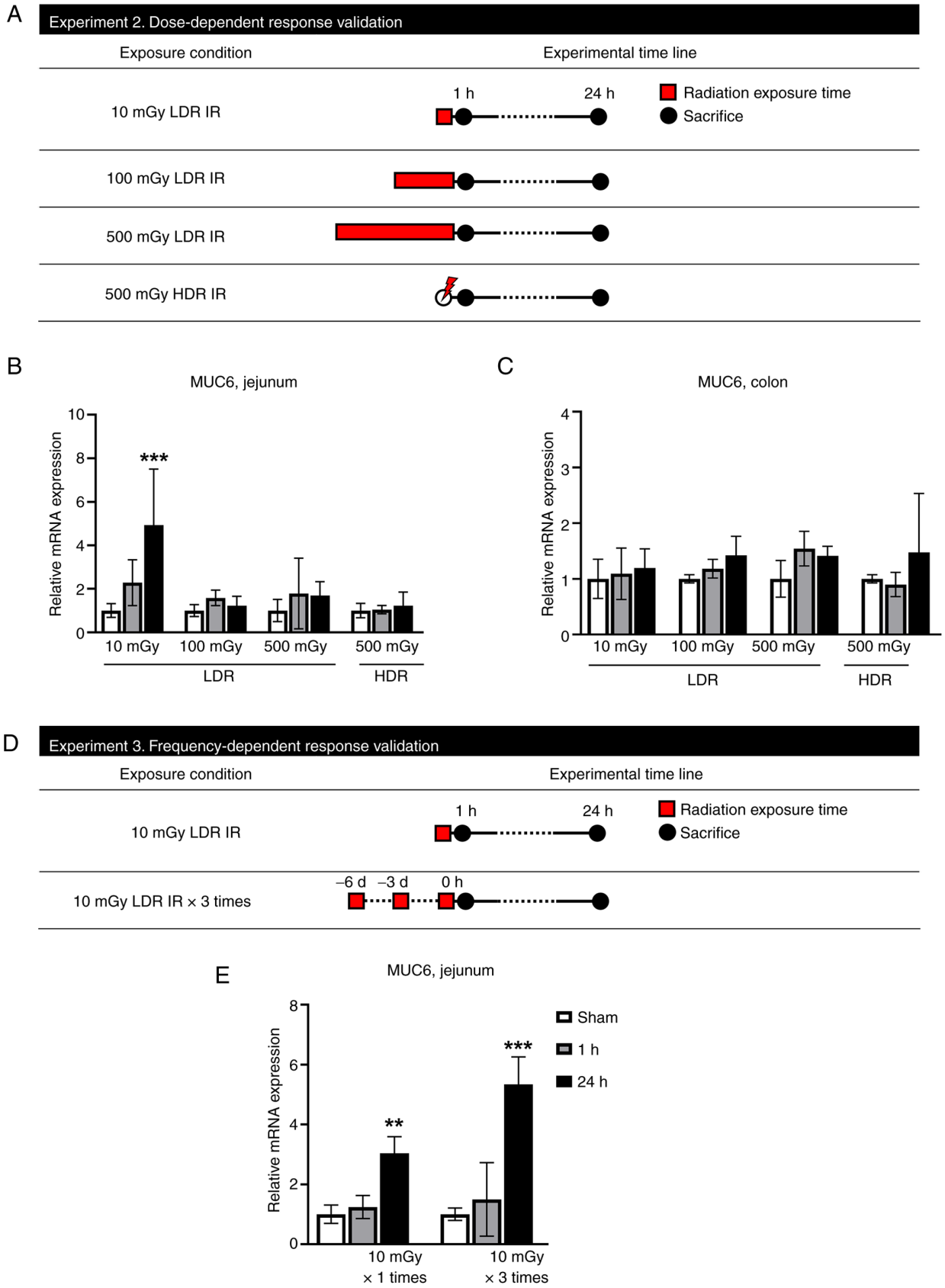

Figure 4. MUC6 mRNA increases in low dose of LDR IR and repeated LDR IR exposure conditions in the jejunum. (A) Schematic diagram of the experimental procedure. In experiment 2, mice exposed to LDR IR with 0, 10, 100, or 500 mGy or HDR IR with 500 mGy, then sacrificed at 1 or 24 h following IR. Red square indicates radiation exposure time; black circles indicate the times of tissue collection from test animals. Changes in the mRNA expression of MUC6 in the intestine of mice exposed to LDR IR. Dose-related changes in MUC6 mRNA expression level in (B) jejunum and (C) colon. (D) Schematic diagram of the experimental procedure. In experiment 3, mice irradiated with sham, 10 mGy once, or 10 mGy three times were sacrificed for tissue sampling at 1 or 24 h following LDR IR (n=3 mice per group). Red square indicates radiation exposure time; black circles indicate the times of tissue collection from test animals. (E) Repetition-related changes in MUC6 mRNA expression level in jejunum. Data are expressed as the mean ± SEM (n=3 mice per group). **P<0.01 and ***P<0.001 vs. the sham group. MUC6, mucin 6; LDR IR, low-dose-rate irradiation; HDR IR, high-dose-rate irradiation.

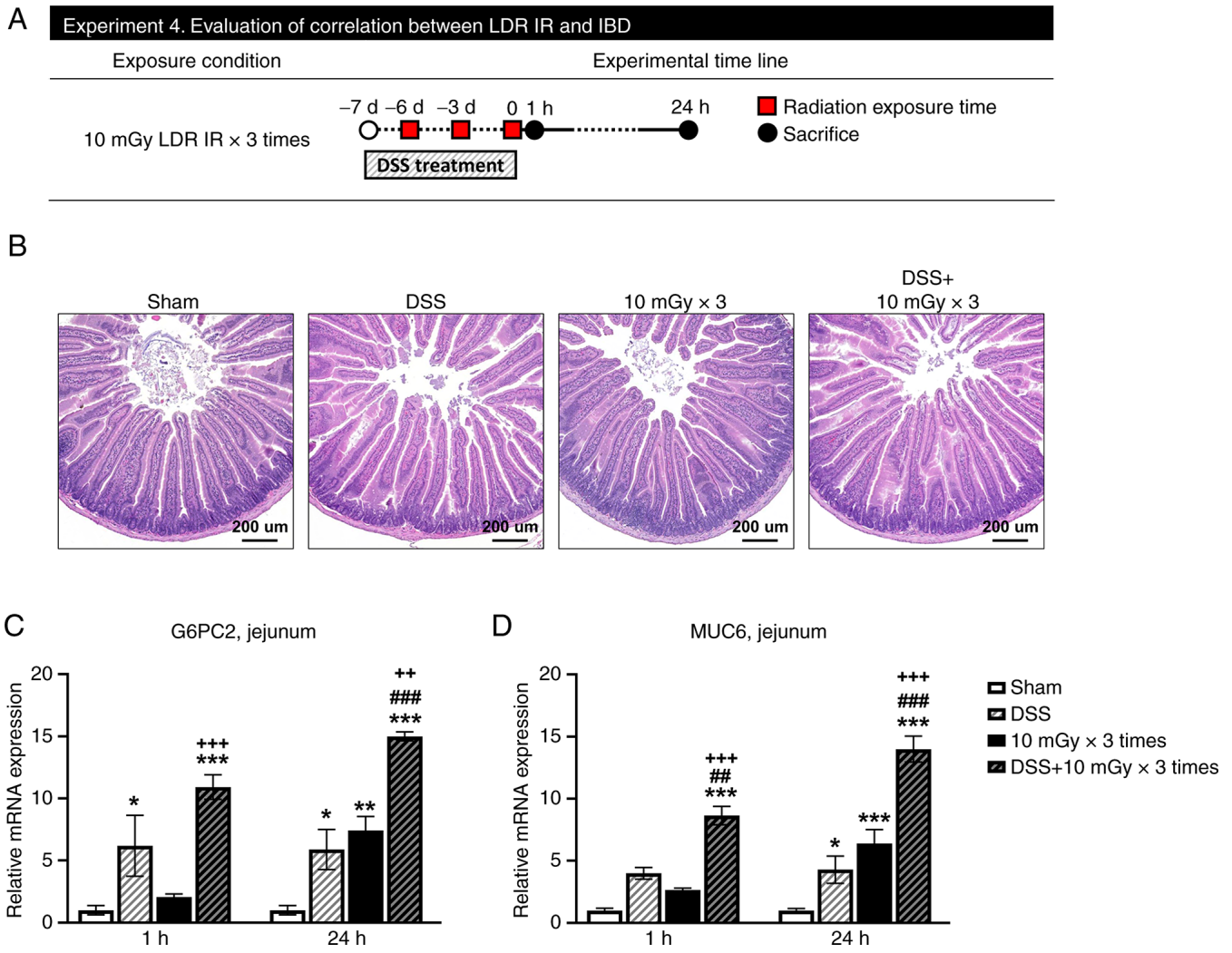

Figure 5. DSS and LDR IR did not alter jejunal morphology but increased G6PC2 and MUC6 mRNA expression. (A) Schematic diagram of the experimental procedure. In experiment 4, DSS-induced IBD model mice irradiated with 10 mGy three times were sacrificed for tissue sampling at 1 or 24 h following LDR IR. Red square indicates radiation exposure time; gray square indicates DSS treatment period; black circles indicate the times of tissue collection from test animals. (B) Representative images of hematoxylin and eosin-stained jejunal sections harvested from vehicle- or DSS-treated mice at 24 h after 10 mGy 3 times LDR IR. Changes in the mRNA expression of (C) G6PC2 and (D) MUC6 in the jejunum of mice exposed to DSS and LDR IR. Data are expressed as the mean ± SEM (n=3 mice per group). *P<0.05, **P<0.01 and ***P<0.001 vs. the sham group; $^{\#\#}$P<0.01 and $^{\#\#\#}$P<0.001 vs. the DSS group; $^{++}$P<0.01 and $^{+++}$P<0.001 vs. the 10 mGy X3 times group. DSS, dextran sodium sulfate; LDR IR, low-dose-rate irradiation; G6PC2, glucose-6-phosphatase catalytic subunit 2; MUC6, mucin 6; IBD, inflammatory bowel disease.

The small intestine is highly vulnerable to radiation (26). The main symptoms of radiation-induced intestinal injury include vomiting, diarrhea, anorexia, systemic infections and, in severe cases, septic shock and death (27). Several research teams are investigating the identification and therapy of the underlying mechanisms responsible for radiation-induced gastrointestinal problems. The influence of the gastrointestinal system on radiation has mainly studied in the jejunum, specifically 3 days after exposure to a radiation dose of 10 Gy (4,28). Radiation causes changes in the structure and function of the intestines, including the death of intestinal crypt cells, disruption of the barrier and inflammation of the mucous membrane, resulting in a decrease in the height of the villi (29). However, the effect of LDR IR on the jejunum remains uncertain.

RNA-seq was used to determine the molecular differences between the jejunum of sham- and LDR IR-exposed mice. Through GO:BP analysis, a notable variation in 12 GO:BP terms was detected 1 h after exposure to 10 mGy irradiation, with the digestion (GO:0007586) showing the most significant change. At 24 h following exposure to 10 mGy irradiation, a notable difference was detected in 14 GO:BP terms, with the adaptive immune response (GO:0002250) being the most significant alteration. Although no common GO:BP term were identified between these two time points, it was found that 23 genes exhibited an expected increase. PCR and western blot analyses confirmed that the gene expressions of G6PC2 and MUC6 were upregulated following irradiation. This study revealed that the gene expressions of G6PC2 and MUC6 increased in response to LDR IR (10 mGy) and their expression further increased when the LDR IR was exposed repeatedly.

G6PC2, known as islet-specific glucose-6-phosphate-catalytic-subunit-related protein (IGRP), is one of three G6PC isoforms that catalyze the hydrolysis of glucose 6-phosphate to glucose and inorganic phosphate. G6PC2 is expressed almost exclusively in pancreatic islet beta cells, which are supposed to act as a negative regulator of the beta cell glucose sensor

glucokinase (30,31). Instead of employing its enzymatic function, G6PC2 acts as a major autoantigen in type I diabetes patients and mouse models of human disease. Studies show that G6PC2 ($IGRP_{206-214}$)-reactive CD8+ T cells may modulate the interaction between type I diabetes and colitis through molecular mimicry in non-obese diabetic (NOD) mice. Antigen mimics from gut microbes could activate or repress G6PC2 ($IGRP_{206-214}$)-reactive CD8+ T cells, resulting in the modulation of type I diabetes and colitis (32,33).

MUC6, an isoform of mucin glycoproteins, is found only in the stomach and duodenum of healthy individuals and generates gel-forming mucin that covers the digestive epithelium (34). Several investigations have found MUC6 in breast mucinous carcinoma, stomach adenocarcinoma, colon neuroendocrine carcinoma and pulmonary adenocarcinoma (34-37). In addition to its association with cancer, MUC6 plays a role in epithelial wound healing after mucosal injury in IBDs, such as Crohn's disease (38).

In the present study, G6PC2 and MUC6 upregulation was observed in the jejunum following exposure to LDR IR, whereas no comparable alteration was observed in the colon. These two genes have been linked to the pathogenesis of IBD, such as colitis (33) and Crohn's disease (38). Therefore, the present study aimed to induce IBD using DSS, a chemical that induces colitis, and to validate the expression of G6PC2 and MUC6 in radiation-exposed jejunum. While the colon is well recognized as the main location of DSS-induced damage, reports indicate that the small intestine, specifically the jejunum-ileum, is also susceptible to slight effects (39). However, in the present study, histological confirmation did not reveal any damage in the jejunum induced by DSS. Although no studies are available on the expression and roles of G6PC2 in the intestine, the results of the present study showed that G6PC2 was expressed in the jejunum and its expression could be enhanced by LDR IR or inflammation (DSS treatment) and more significantly when both were applied simultaneously. Crohn's disease can affect any part of the gastrointestinal tract. Although ulcerative colitis (UC) generally occurs in the colon, it can also affect the part of the intestine during severe colitis (40). Thus, G6PC2 can be induced by LDR IR- and/or disease-associated inflammation and may play some role in modulating inflammation in the intestine and type I diabetes. At present, it is not known whether proteins of any microbes in the intestine can act as antigenic mimics of G6PC2-reactive CD8+ T cells. The possibility and role of LDR IR-induced G6PC2 in the intestine may need further investigation. Consistent with these reports, the results of the present study showed that MUC6 expression in the intestine can be enhanced by LDR IR- or inflammation (DSS treatment). Furthermore, simultaneous treatment with both stimuli can further increase its expression. MUC6 may play protective roles in LDR IR- -induced, or disease- and cancer-associated inflammation. However, it may be possible that inflammation-induced MUC6 expression in unexpected regions contributes to cancer development. Thus, further investigations on the roles of enhanced MUC6 expression in inflammatory environments are required.

During the present study, it was shown that when exposed to LDR IR, the genes associated with inflammation in the intestines, namely G6PC2 and MUC6, were increased in the jejunum. Furthermore, it was determined that this rise occurred under repeated exposure to LDR IR. Moreover, these genes exhibited a further increase in the presence of pre-existing enteritis. Nevertheless, due to the absence of clinical symptoms or morphological alterations in the jejunum, establishing a clear relationship between the G6PC2 and MUC6 genes and intestinal inflammation could not be achieved. Future research should modify these irradiation settings and expand the post-irradiation period to validate the long-term alteration pattern in the jejunum.

The present study revealed particular genes that were upregulated by LDR IR. It is recognized that in gene expression analysis, it is essential to take into account both upregulated and downregulated genes. The present study tried to validate thoroughly the RNA-seq results with RT-qPCR but encountered difficulties in confirming the downregulated genes. Despite attempts to resolve and deal with these problems, achieve reliable validation for the downregulated genes could not be achieved in the present study. Therefore, it was decided to focus on reporting and discussing the confirmed upregulated genes in the results. The limitation of excluding downregulated genes from the validation procedure is recognized and the valuable insights that may have been obtained by investigating them. Although limited, the present study provided useful insights into the upregulated gene expression alterations in the small intestine under LDR IR.

Acknowledgements

Not applicable.

Funding

The present study was funded by the Dongnam Institute of Radiological & Medical Sciences (DIRAMS) grant funded by the Korean government (MSIT), grant nos. 50496-2017 and 50491-2021. It was also supported by grants from the National Research Foundation (grant nos. NRF-2020M2C8A2069337 and NRF-2020R1A2C1004272) funded by the Ministry of Science and ICT (MSIT), Republic of Korea.

Availability of data and materials

The metagenomic sequencing data may be found in the sequence read archive (SRA) database under accession number PRJNA 1086250 or at the following URL: ncbi.nlm.nih.gov/sra/PRJNA1086250. The data generated in the present study may be requested from the corresponding author.

Authors' contributions

CGL and JSK conceived the present study. SK, MJB and YS performed the investigations. MJB, WSJ, CM and HJL were involved in data analysis and interpretation. MKK, HJK, YRK, BJ and JL curated the data by collecting, arranging and processing the data. CGL and JSK confirm the authenticity of all the raw data. SK, MJB, CGL and JSK wrote the original draft. SK and JSK reviewed and edited the manuscript. All authors have read and approved the final version of the manuscript.

Ethics approval and consent to participate

All experimental procedures were approved by the Institutional Animal Care and Use Committee of Dongnam Institute of Radiological and Medical Sciences (DIRAMS; approval nos. DI-2015-002 and DI-2021-002) and the animals were cared for in accordance with the NIH Guide for the Care and Use of Laboratory Animals.

Patient consent for publication

Not applicable.

Competing interests

The authors declare that they have no competing interests.

References

1. Hall EJ: Weiss lecture. The dose-rate factor in radiation biology. Int J Radiat Biol 59: 595-610, 1991.
2. Narendran N, Luzhna L and Kovalchuk O: Sex difference of radiation response in occupational and accidental exposure. Front Genet 10: 260, 2019.
3. Nam HH, Kang S, Seo YS, Lee J, Moon BC, Lee HJ, Lee JH, Kim B, Lee S and Kim JS: Protective effects of an aqueous extract of Protaetia brevitarsis seulensis larvae against radiation-induced testicular injury in mice. Food Sci Nutr 10: 3969-3978, 2022.
4. Kang S, Lee AY, Nam HH, Lee SI, Kim HY, Lee JM, Moon C, Shin IS, Chae SW, Lee JH, *et al*: Protective effect of bojungikki-tang against radiation-induced intestinal injury in mice: Experimental verification and compound-target prediction. Evid Based Complement Alternat Med 2023: 5417813, 2023.
5. Lee HJ, Son Y, Lee M, Moon C, Kim SH, Shin IS, Yang M, Bae S and Kim JS: Sodium butyrate prevents radiation-induced cognitive impairment by restoring pCREB/BDNF expression. Neural Regen Res 14: 1530-1535, 2019.
6. Ren H, Shen J, Tomiyama-Miyaji C, Watanabe M, Kainuma E, Inoue M, Kuwano Y and Abo T: Augmentation of innate immunity by low-dose irradiation. Cell Immunol 244: 50-56, 2006.
7. Schultz CH, Fairley R, Murphy LS and Doss M: The risk of cancer from CT scans and other sources of low-dose radiation: A critical appraisal of methodologic quality. Prehosp Disaster Med 35: 3-16, 2020.
8. Hong JY, Han K, Jung JH and Kim JS: Association of exposure to diagnostic low-dose ionizing radiation with risk of cancer among youths in South Korea. JAMA Netw Open 2: e1910584, 2019.
9. Gong EJ, Shin IS, Son TG, Yang K, Heo K and Kim JS: Low-dose-rate radiation exposure leads to testicular damage with decreases in DNMT1 and HDAC1 in the murine testis. J Radiat Res 55: 54-60, 2014.
10. Kang S, Lee HJ, Son Y, Bae MJ, Jo WS, Park JH, Jeong S, Moon C, Shin IS, Lee CG and Kim JS: Low-dose-rate gamma radiation aggravates titanium dioxide nanoparticle-induced lung injury in mice. Mol Cell Toxicol 20: 389-398, 2024.
11. Jo WS, Kang S, Jeong SK, Bae MJ, Lee CG, Son Y, Lee HJ, Jeong MH, Kim SH, Moon C, *et al*: Low dose rate radiation regulates M2-like macrophages in an allergic airway inflammation mouse model. Dose Response 20: 15593258221117349, 2022.
12. Son Y, Lee CG, Kim JS and Lee HJ: Low-dose-rate ionizing radiation affects innate immunity protein IFITM3 in a mouse model of Alzheimer's disease. Int J Radiat Biol 99: 1649-1659, 2023.
13. Bachmann R, Heinzelmann F, Müller AC, Ladurner R, Schneider CC, Königsrainer A and Zdichavsky M: Laparoscopic pelvic mesh placement with closure of pelvic floor entrance to prevent small intestine radiation trauma-a retrospective cohort analysis. Int J Surg 23: 62-67, 2015.
14. Moussa L, Usunier B, Demarquay C, Benderitter M, Tamarat R, Sémont A and Mathieu N: Bowel radiation injury: Complexity of the pathophysiology and promises of cell and tissue engineering. Cell Transplant 25: 1723-1746, 2016.
15. Loge L, Florescu C, Alves A and Menahem B: Radiation enteritis: Diagnostic and therapeutic issues. J Visc Surg 157: 475-485, 2020.
16. National Research Council (US) Committee for the Update of the Guide for the Care and Use of Laboratory Animals. Guide for the care and use of laboratory animals. 8th edition. The National Academies Press: Washington, DC, USA, 2011.
17. Siriarchavatana P, Ayers JD and Kendall LV: Anesthetic activity of alfaxalone compared with ketamine in mice. J Am Assoc Lab Anim Sci 55: 426-430, 2016.
18. Kim JS, Ryoo SB, Heo K, Kim JG, Son TG, Moon C and Yang K: Attenuating effects of granulocyte-colony stimulating factor (G-CSF) in radiation induced intestinal injury in mice. Food Chem Toxicol 50: 3174-3180, 2012.
19. Kang S, Son Y, Shin IS, Moon C, Lee MY, Lim KS, Park SJ, Lee CG, Jo WS, Lee HJ and Kim JS: EFFECT of abdominal irradiation in mice model of inflammatory bowel disease. Radiat Prot Dosimetry 199: 564-571, 2023.
20. Kechin A, Boyarskikh U, Kel A and Filipenko M: cutPrimers: A new tool for accurate cutting of primers from reads of targeted next generation sequencing. J Comput Biol 24: 1138-1143, 2017.
21. Dobin A, Davis CA, Schlesinger F, Drenkow J, Zaleski C, Jha S, Batut P, Chaisson M and Gingeras TR: STAR: Ultrafast universal RNA-seq aligner. Bioinformatics 29: 15-21, 2013.
22. Anders S and Huber W: Differential expression analysis for sequence count data. Genome Biol 11: R106, 2010.
23. Heinz S, Benner C, Spann N, Bertolino E, Lin YC, Laslo P, Cheng JX, Murre C, Singh H and Glass CK: Simple combinations of lineage-determining transcription factors prime cis-regulatory elements required for macrophage and B cell identities. Mol Cell 38: 576-589, 2010.
24. Tripathi S, Pohl MO, Zhou Y, Rodriguez-Frandsen A, Wang G, Stein DA, Moulton HM, DeJesus P, Che J, Mulder LCF, *et al*: Meta- and orthogonal integration of influenza 'OMICs' data defines a role for UBR4 in virus budding. Cell Host Microbe 18: 723-735, 2015.
25. Livak KJ and Schmittgen TD: Analysis of relative gene expression data using real-time quantitative PCR and the 2(-Delta Delta C(T)) method. Methods 25: 402-408, 2001.
26. Guo J, Liu Z, Zhang D, Chen Y, Qin H, Liu T, Liu C, Cui J, Li B, Yang Y, *et al*: TLR4 agonist monophosphoryl lipid a alleviated radiation-induced intestinal injury. J Immunol Res 2019: 2121095, 2019.
27. Lu L, Jiang M, Zhu C, He J and Fan S: Amelioration of whole abdominal irradiation-induced intestinal injury in mice with 3,3'-Diindolylmethane (DIM). Free Radic Biol Med 130: 244-255, 2019.
28. Livanova AA, Fedorova AA, Zavirsky AV, Bikmurzina AE, Krivoi II and Markov AG: Dose and time dependence of functional impairments in rat jejunum following ionizing radiation exposure. Physiol Rep 9: e14960, 2021.
29. Wang J, Zheng H, Kulkarni A, Ou X and Hauer-Jensen M: Regulation of early and delayed radiation responses in rat small intestine by capsaicin-sensitive nerves. Int J Radiat Oncol Biol Phys 64: 1528-1536, 2006.
30. Hutton JC and O'Brien RM: Glucose-6-phosphatase catalytic subunit gene family. J Biol Chem 284: 29241-29245, 2009.
31. Boortz KA, Syring KE, Pound LD, Mo H, Bastarache L, Oeser JK, McGuinness OP, Denny JC and O'Brien RM: Effects of G6pc2 deletion on body weight and cholesterol in mice. J Mol Endocrinol 58: 127-139, 2017.
32. Tai N, Peng J, Liu F, Gulden E, Hu Y, Zhang X, Chen L, Wong FS and Wen L: Microbial antigen mimics activate diabetogenic CD8 T cells in NOD mice. J Exp Med 213: 2129-2146, 2016.
33. Hebbandi Nanjundappa R, Ronchi F, Wang J, Clemente-Casares X, Yamanouchi J, Sokke Umeshappa C, Yang Y, Blanco J, Bassolas-Molina H, Salas A, *et al*: A gut microbial mimic that hijacks diabetogenic autoreactivity to suppress colitis. Cell 171: 655-667.e17, 2017.
34. Dwertmann Rico S, Schliesser SJA, Gorbokon N, Dum D, Menz A, Büscheck F, Hinsch A, Lennartz M, von Bargen C, Bawahab AA, *et al*: Pattern of MUC6 expression across 119 different tumor types: A tissue microarray study on 15 412 tumors. Pathol Int 73: 281-296, 2023.
35. Kufe DW: Mucins in cancer: Function, prognosis and therapy. Nat Rev Cancer 9: 874-885, 2009.
36. Bhatia R, Gautam SK, Cannon A, Thompson C, Hall BR, Aithal A, Banerjee K, Jain M, Solheim JC, Kumar S and Batra SK: Cancer-associated mucins: Role in immune modulation and metastasis. Cancer Metastasis Rev 38: 223-236, 2019.

37. Hamamoto A, Abe Y, Nishi M, Fujimori S, Ohnishi Y, Yamazaki H, Oida Y, Miyazaki N, Inada KI, Ueyama Y, *et al*: Aberrant expression of the gastric mucin MUC6 in human pulmonary adenocarcinoma xenografts. Int J Oncol 26: 891-896, 2005.
38. Buisine MP, Desreumaux P, Leteurtre E, Copin MC, Colombel JF, Porchet N and Aubert JP: Mucin gene expression in intestinal epithelial cells in Crohn's disease. Gut 49: 544-551, 2001.
39. Geier MS, Smith CL, Butler RN and Howarth GS: Small-intestinal manifestations of dextran sulfate sodium consumption in rats and assessment of the effects of Lactobacillus fermentum BR11. Dig Dis Sci 54: 1222-1228, 2009.
40. Mourad FH, Barada KA and Saade NE: Impairment of small intestinal function in ulcerative colitis: Role of enteric innervation. J Crohns Colitis 11: 369-377, 2017.